Biochemical Pharmacology, Vol. 60, pp. 7–17, 2000.

ISSN 0006-2952/00/$–see front matter
PII S0006-2952(00)00301-4

Stereoselective Sulfoxidation of Sulindac Sulfide by Flavin-Containing Monooxygenases

COMPARISON OF HUMAN LIVER AND KIDNEY MICROSOMES AND MAMMALIAN ENZYMES

Mitchell A. Hamman, Barbara D. Haehner-Daniels,* Steven A. Wrighton,† Allan E. Rettie‡ and Stephen D. Hall*§*

*Division of Clinical Pharmacology, Indiana University School of Medicine, Indianapolis, IN 46202; ‡Department of Medicinal Chemistry, University of Washington, Seattle, WA 98195; and †Eli Lilly & Company, Lilly Corporate Center, Indianapolis, IN 46202, U.S.A.

ABSTRACT. The stereoselective sulfoxidation of the pharmacologically active metabolite of sulindac, sulindac sulfide, was characterized in human liver, kidney, and cDNA-expressed enzymes. Kinetic parameter estimates (pH = 7.4) for sulindac sulfoxide formation in human liver microsomes (N = 4) for *R*- and *S*-sulindac sulfoxide were V_{max} = 1.5 ± 0.50 nmol/min/mg, K_m = 15 ± 5.1 μM; and V_{max} = 1.1 ± 0.36 nmol/min/mg, K_m = 16 ± 6.1 μM, respectively. Kidney microsomes (N = 3) produced parameter estimates (pH = 7.4) of V_{max} = 0.9 ± 0.29 nmol/min/mg, K_m = 15 ± 2.9 μM; V_{max} = 0.5 ± 0.21 nmol/min/mg, K_m = 22 ± 1.9 μM for R- and *S*-sulindac sulfoxide, respectively. In human liver and flavin-containing monooxygenase 3 (FMO3) the V_{max} for *R*-sulindac sulfoxide increased 60–70% at pH = 8.5, but for *S*-sulindac sulfoxide was unchanged. In fourteen liver microsomal preparations, significant correlations occurred between *R*-sulindac sulfoxide formation and either immunoquantified FMO or nicotine *N*-oxidation (r = 0.88 and 0.83; $P < 0.01$). The *R*- and *S*-sulindac sulfoxide formation rate also correlated significantly (r = 0.85 and 0.75; $P < 0.01$) with immunoquantified FMO in thirteen kidney microsomal samples. Mild heat deactivation of microsomes reduced activity by 30–60%, and a loss in stereoselectivity was observed. Methimazole was a potent and nonstereoselective inhibitor of sulfoxidation in liver and kidney microsomes. *n*-Octylamine and membrane solubilization with lubrol were potent and selective inhibitors of *S*-sulindac sulfoxide formation. cDNA-expressed CYPs failed to appreciably sulfoxidate sulindac sulfide, and CYP inhibitors were ineffective in suppressing catalytic activity. Purified mini-pig liver FMO1, rabbit lung FMO2, and human cDNA-expressed FMO3 efficiently oxidized sulindac sulfide with a high degree of stereoselectivity towards the *R*-isomer, but FMO5 lacked catalytic activity. The biotransformation of the sulfide to the sulfoxide is catalyzed predominately by FMOs and may prove to be useful in characterizing FMO activity. BIOCHEM PHARMACOL **60**;1:7–17, 2000. © 2000 Elsevier Science Inc.

KEY WORDS. sulindac; enantiomers; flavin-containing monooxygenase; sulfoxidation; microsomes; drug metabolism

Sulindac, *Z*-5-fluoro-2-methyl-1-[*p*-(methylsulfinyl)benzyl-diene]indene-3-acetic acid, is a NSAID‖ that contains a chiral sulfoxide moiety and is administered clinically as a racemate. SOX is reduced reversibly *in vivo* to the pharmacologically active metabolite SID, which is primarily responsible for the inhibition of cyclooxygenase [1–3]. Additionally, SOX is oxidized to an inactive sulfone metabolite (Fig. 1). We and others have observed in clinical studies that serum concentrations of both SOX and SID are elevated in the elderly, thus enhancing the likelihood of NSAID-induced toxicity in this high-risk group of patients [4–6]. Both acutely and chronically dosed volunteers showed a distinct stereoselective enrichment of *R*-SOX in serum and urine [5, 7].

The use of SOX in the management of chronic pain and inflammation has been proposed to have fewer deleterious renal side-effects, such as increased sodium and potassium retention, nephrotic syndrome, and decreased glomerular filtration rate, than are associated with other NSAIDs [8–11]. Renal tissue is capable of oxidizing the active SID metabolite to the inactive sulfoxide [12]. Thus, the hypothesis was proposed that the "renal sparing" effect of sulindac is due to the conservation of the prostaglandin synthesis required to maintain normal kidney function. The characterization of this protective pathway may allow the renal sparing properties to be extended to other NSAIDs.

§ Corresponding author: Stephen D. Hall, Ph.D., Clinical Pharmacology, 320 OPW Wishard Memorial Hospital, 1001 West Tenth Street, Indianapolis, IN 46202-2879. Tel. (317) 630-8795; FAX (317) 630-8185; E-mail: SDHALL@IUPUI.EDU

‖ *Abbreviations*: NSAID, nonsteroidal anti-inflammatory drug; FMO, flavin-containing monooxygenase; CYP, cytochrome P450; SOX, sulindac sulfoxide; and SID, sulindac sulfide.

Received 16 August 1999; accepted 11 November 1999.

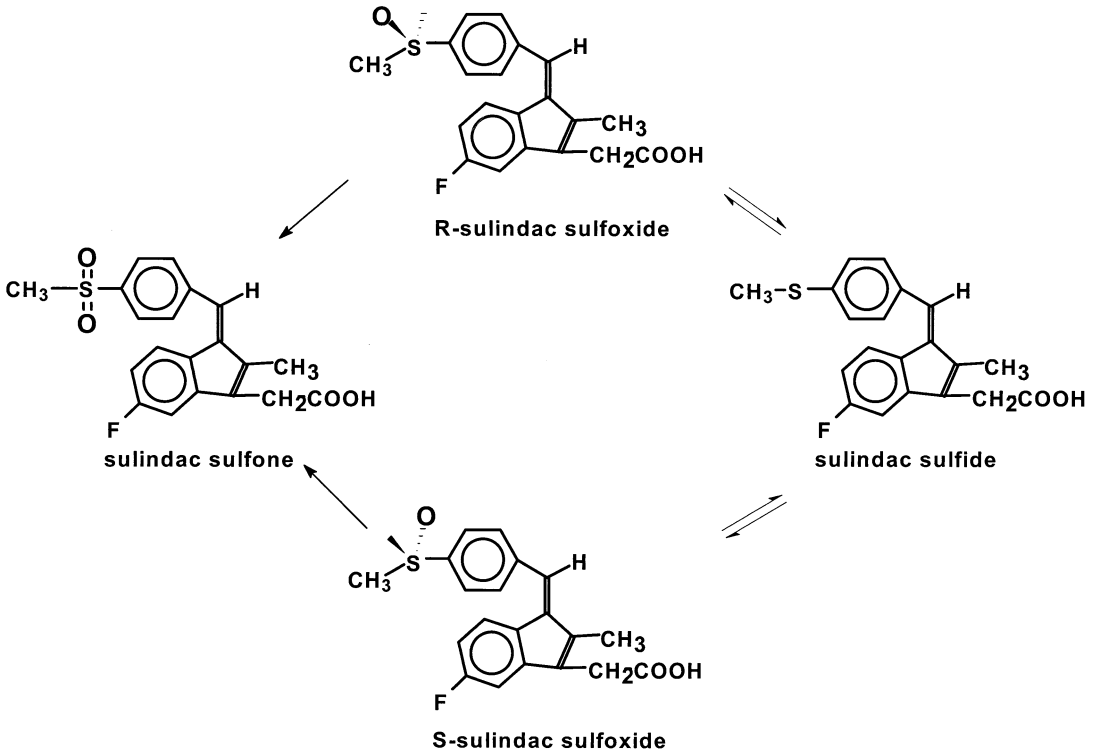

FIG. 1. Oxidative and reductive human biotransformations of sulindac *in vivo*. Racemic sulindac sulfoxide, a prodrug, is reversibly reduced to the active sulfide metabolite, which is reoxidized to either the *R*- or *S*-sulfoxide enantiomer. The sulfoxides are also irreversibly oxidized further to a sulfone metabolite. The reduction of the sulfoxides to sulfide is a nonmicrosomal process, and therefore is not a confounding parameter in determining microsomal oxidation.

The oxidation of the prochiral SID has been observed for both FMO (EC 1.14.13.8) in mammalian tissues and CYP with rat liver microsomes [13, 14]. For example, the conversion of the sulfide to sulfoxide by purified hog liver FMOs proved to be highly efficient and stereoselective for *R*-SOX [14]. To date, five forms of FMO have been identified, but the human complement of FMOs has not been fully characterized [15]. Differences in catalytic activity and stereoselectivity between human hepatic, fetal, and renal forms were noted using the prototypic FMO substrate *p*-tolyl methyl sulfide, but in each case formation of the *R*-enantiomer was favored [16, 17]. Therefore, we have characterized the involvement of FMOs and CYPs in the biotransformation of SID in human liver and kidney microsomes, and cDNA-expressed microsomes with an emphasis on stereochemistry. In addition to providing a better understanding of the stereoselective disposition and renal effects of sulindac *in vivo*, these studies examined the utility of SID as a probe for FMO enzymes *in vitro*.

MATERIALS AND METHODS

Materials

SOX and SID were obtained from Merck Sharp & Dohme. Indomethacin, troleandomycin, quinidine, lauric acid, diethyldithiocarbamic acid, methimazole, *n*-octylamine, lubrol PX, and coumarin were purchased from the Sigma Chemical Co. Sulfaphenazole was obtained from Ciba-Geigy. Furafylline was acquired from Research Biochemicals International. *S*-Mephenytoin was purchased from Ultrafine Chemicals. Microsomes from B-lymphoblastoid cell lines expressing CYP1A2, CYP2A6, CYP2C8, CYP2C9-Arg144, CYP2C19, CYP2D6, CY2E1, CYP3A4, and CYP4A11, control microsomes, human cDNA-expressed FMO3, and FMO5 from baculovirus-transfected insect cells (Supersomes) were acquired from Gentest. All other chemicals were purchased from commercial sources, and were of the highest purities available.

A bank of fourteen liver samples (designated HL-A through HL-N), which have been characterized for CYP and FMO catalytic activities and immunoquantified protein levels, was obtained under protocols approved by the Medical College of Wisconsin [18]. Two additional livers (designated IUL11 and IUL12) and thirteen kidney samples (designated HK-A through HK-M) were obtained under a protocol approved by the Institutional Review Board of Indiana University Medical Center. Microsomes were prepared by differential centrifugation using conventional methods. The microsomes were stored in a 100 mM potassium phosphate buffer, pH 7.4, containing 1 mM EDTA, 20% glycerol, 20 μM butylated hydroxytoluene, 100 μM phenylmethylsulfonyl fluoride, and stored at −80°. Microsomal protein concentrations were measured by the

method of Lowry *et al.* [19]. Mini-pig liver FMO1 and rabbit lung FMO2 were purified from tissues as previously reported [16, 20].

Immunoquantitation

Liver and kidney microsomal FMO was quantified by SDS–PAGE electrophoresis (50 μg microsomal protein) followed by immunoblotting on nylon membranes with a New Zealand White rabbit polyclonal antibody raised against FMO1 and developed with horseradish peroxidase-conjugated goat secondary antibody [16]. Chemiluminescence was quantified with a BioImage scanning densitometer (Beckman). The relative liver microsomal FMO concentration in the bank of fourteen human livers has been previously reported extensively [18, 21, 22].

Microsomal Incubations

Microsomal incubations consisted of sodium phosphate buffer (100 mM, pH 7.4, 0.1 mM EDTA) and 0.1 to 0.5 mg protein or 150 pmol rabbit FMO1/2 or cDNA-expressed human FMO3/5. SID was added in 5 μL of methanol, and the mixture was preincubated for 2 min. The reaction was initiated with the addition of 1 μmol NADPH to give a final volume of 1 mL and was allowed to continue for 5–20 min. Control microsomes were incubated with SID, protein, and no NADPH. Substrate concentration dependence was determined with a SID concentration range of 1 to 300 μM. Putative inhibitors were preincubated along with substrate for 2 min with the exceptions of troleandomycin and furafylline, which were preincubated with NADPH for 20 min prior to initiation with SID. To characterize the effects of heat deactivation, microsomes were warmed to 55° for 90 sec, and then cooled on ice prior to use [23]. The reactions were terminated with the addition of 1 mL ethyl acetate and stored on ice.

HPLC Analyses

The concentration of SOX was determined by reverse phase chromatography. Following termination of enzyme incubations, 50 μL of indomethacin (50 ng/mL) internal standard and 50 μL of 50% phosphoric acid were added followed by extraction with 3.5 mL of ethyl acetate. After centrifugation at 2000 *g* for 10 min, the organic layer was removed and evaporated to dryness with a vacuum concentrator and reconstituted with 100 μL mobile phase (see below), from which 50–75 μL was injected. The separation was achieved with a 5-μm octyl column (100 × 4.6 mm i.d., Brownlee Spherisorb, Applied Biosystems) eluted isocratically (mobile phase: 50 mM potassium phosphate, pH 3/acetonitrile; 50/50, v/v) at 0.8 mL/min and monitored by UV absorbance at 360 nm. The retention times for SOX, indomethacin, and SID were 2.7, 3.8, and 6.9 min, respectively. The interday coefficient of variation for SOX (200 pmol) was 7.4%. The peak identified as SOX, in both standards and samples, was collected for determination of enantiomeric composition. The fraction containing SOX was evaporated and reconstituted with 100 μL of chiral chromatography mobile phase described below.

SOX ENANTIOMERS. Enantiomeric separation was accomplished with chiral recognition phase chromatography consisting of a 7-μm particle size BSA column (150 × 4.6 mm i.d., Macherey-Nagel Resolvosil, Applied Biosystems) eluted isocratically (mobile phase: 0.1 M sodium phosphate, 0.1 M sodium acetate, pH 7.8/*n*-propanol; 96/4, v/v) at 1 mL/min and monitored at 280 nm. Complete resolution of SOX enantiomers was obtained with this method with retention times of 10.5 and 17.8 min and a resolution factor of 2.4. Absolute configuration assignment is detailed later in the text. The injection of multiple concentrations (100–10,000 pmol) of an authentic racemic standard gave virtually identical peak areas of each enantiomer, indicating that the chromatography system is suitable for quantification. Although sulfoxide enantiomers are for the most part stable, the extraction and reverse phase chromatography were tested for possible inversion. Deactivated (heated at 90° for 3 min) rat liver microsomal reaction mixtures were spiked with *R*- or *S*-SOX and assayed as described above; no detectable inversion occurred. Therefore, the fractional response for each enantiomer and the total concentration of SOX gave the enantiomer concentration.

CHIRAL STATIONARY PHASE CHROMATOGRAPHY. To assign an absolute configuration to the stereoisomers of SOX, a π donor/acceptor chiral stationary phase column was employed. The (*R, R*) WHELK-01 (250 × 4.6 mm i.d., Regis Chemical Co.) is a silica-based column that is covalently bonded with a 4-(3,5-dinitrobenzamido)tetrahydrophenanthracene moiety and fixed chiral centers. This column has proved to be useful in the separations of chiral compounds that have aromatic rings to donate π electrons. *R*- and *S*-SOX were resolved by eluting the column with a mobile phase consisting of hexane/absolute ethanol/trifluoroacetic acid, 60/40/1 (by vol.), at 1 mL/min and monitoring UV absorbance at 360 nm. The stereoisomer retention times were 10.5 and 12.8 min, respectively. The prototypic FMO substrate, *p*-tolyl methyl sulfide, when biotransformed by purified hog liver FMO, yielded as the major product *R* (+)-*p*-tolyl methyl sulfoxide, which on this system is the earlier eluting enantiomer. Previously, it was also demonstrated that the purified hog liver FMO converted SID predominately to (+)-SOX [14], which is the earlier eluting enantiomer in both WHELK and BSA chromatography. The oxidized component on SID and the structure of *p*-tolyl methyl sulfide are similar, and their predominant products have the same optical rotation. Additionally, for most chiral compounds separated by the (*R, R*) WHELK-01 column, the *R*-enantiomer elutes first. Combining all the observations together, it seems reasonable to assume that the earlier eluting component of the

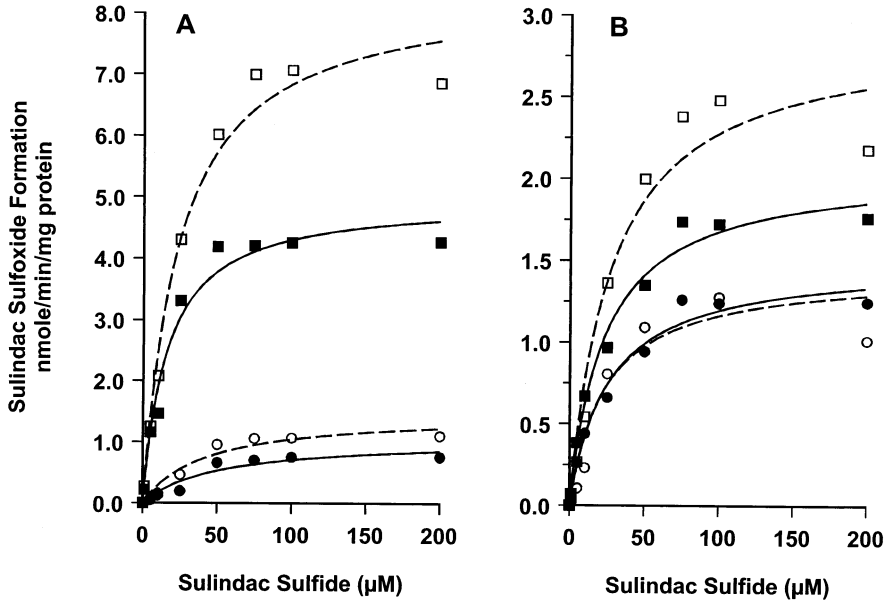

FIG. 2. Dependence of the rate of formation of *R*-SOX (squares) and *S*-SOX (circles) on SID concentration and pH (pH = 7.4, closed symbols; pH = 8.5, open symbols) for (A) cDNA-expressed FMO3, and (B) human liver IUL11. Lines of best fit were determined by nonlinear regression of untransformed data.

BSA chromatography is *R* (+)-SOX and the later is *S* (−)-SOX.

Data Analysis

Enzyme kinetic parameters were determined by nonlinear regression with PCNONLIN (version 4.0, SCI Software). Substrate concentration dependence was fitted to the simple one-enzyme Michaelis–Menten equation. The model was selected based on inspection of residuals, residual sums of squares, magnitude of the standard error in parameter estimates, and visual inspection of Eadie–Hofstee plots [24]. Correlation coefficients and corresponding statistical significance were calculated by conventional methods (PC-SAS, SAS Institute, Inc.). All measurements were the average of duplicate determinations.

RESULTS

Time dependence in the rate of formation of *R*- and *S*-SOX was examined at 30 μM SID and 0.2 mg protein (pH = 7.4) in liver and kidney tissue microsomal samples. Formation rates with human liver microsomes were linear with respect to time for *R*- and *S*-SOX for up to 30 and 20 min, respectively. Control microsomes containing SID with no NADPH showed a detectable but below quantitative level of formation of SOXs. In kidney microsomal samples, metabolite formation was linear for 20 min for both SOX enantiomers. Lastly, formation of SOXs with cDNA-expressed FMO3 (0.1 mg protein) and 30 μM SID was linear with respect to time for 10 min. The rates of formation of SOXs as a function of SID concentration are presented in Fig. 2, and the corresponding parameter estimates are given in Table 1. The intrinsic clearance for *R*-SOX was 1.6 times greater than *S*-SOX formation in liver and kidney microsomes at pH 7.4.

FMO-catalyzed reactions are generally sensitive to pH and thermal stresses above 40° [23]. Raising the incubation buffer pH to 8.5, optimal for FMO-mediated reactions, resulted in a 70 and 59% increase in the maximal *R*-SOX formation rate with liver microsomes and cDNA-expressed FMO3, respectively (Table 1 and Fig. 2). In contrast, *S*-SOX formation was affected marginally by the elevation of pH. Liver microsomes (HL-E) warmed to 55° for 90 sec prior to use showed an approximately 44% decrease in V_{max} of *R*-SOX but little change in *S*-SOX formation rate. Similarly, *R*-SOX formation rate in kidney microsomes (HK-J) was thermally labile with a 58% decrease upon warming, and no change in formation of the *S*-enantiomer (Table 1). These data clearly indicate that *S*-SOX formation in human microsomal preparations is insensitive to conventional modulators of FMO activity.

Figure 3A illustrates the effects of selective inhibitors of CYPs on the conversion of SID (30 μM) to SOX in human liver HL-E (0.2 mg protein). Coumarin (1 mM: CYP2A6), sulfaphenazole (5 μM: CYP2C9), *S*-mephenytoin (0.5 mM: CYP2C19), diethyldithiocarbamic acid (0.3 mM: CYP2E1), and quinidine (0.3 mM: CYP2D6) did not inhibit SID sulfoxidation. Furafylline (0.1 mM: CYP1A2) and troleandomycin (0.1 mM: CYP3A4) caused a minor reduction in the rate of *R*-SOX formation. Enzyme solubilization with the detergent lubrol and incubation with the nonspecific CYP450 inhibitor *n*-octylamine produced a dramatic reduction of the rate of *S*-SOX formation but not *R*-SOX formation (Fig. 3B). Methimazole, an inhibitor of FMO, was a potent but nonstereoselective inhibitor of SOX

TABLE 1. Parameters (± SEM determined by nonlinear regression) characterizing the substrate concentration dependence of the rates of *R*- and *S*-sox formation from SID in human liver, kidney, and cDNA-expressed human FMO3 at pH 7.4 or 8.5 and heat deactivation

	R-SOX			*S*-SOX		
	V_{max} (nmol/min/mg)	K_m (μM)	Cl_{int} (μL/min)	V_{max} (nmol/min/mg)	K_m (μM)	Cl_{int} (μL/min)
Liver, pH = 7.4						
HL-E	1.6 ± 0.90	9 ± 2.3	180	1.1 ± 0.67	12 ± 3.2	92
HL-1	0.7 ± 0.50	13 ± 4.6	54	0.5 ± 0.42	11 ± 5.2	45
IU11	2.1 ± 0.94	23 ± 3.6	91	1.5 ± 0.90	26 ± 5.1	58
IU12	1.6 ± 0.95	14 ± 3.4	114	1.1 ± 0.63	13 ± 3.2	85
Mean	1.5	15	110	1.1	16	70
SD	0.50	5.1	45.8	0.36	6.1	19.2
Liver heat deactivation, 55° 90 sec						
HL-E	0.9 ± 0.42	13 ± 3.3	69	0.9 ± 0.38	11 ± 3.6	82
Liver pH = 8.5						
HL-E	2.1 ± 0.14	16 ± 4.2	131	1.1 ± 0.11	16 ± 6.1	69
HL-I	1.0 ± 0.08	19 ± 6.5	53	0.5 ± 0.06	15 ± 8.1	33
IU11	2.9 ± 0.28	28 ± 8.7	104	1.4 ± 0.19	24 ± 10.8	58
IU12	2.6 ± 0.29	27 ± 10.0	96	1.3 ± 0.12	24 ± 9.7	54
Mean	2.2	23	96	1.1	20	54
SD	0.72	5.1	28.0	0.35	4.3	13.1
FMO3, pH = 7.4	5.0 ± 0.27	16 ± 3.4	313	1.1 ± 0.18	51 ± 22.0	22
FMO3, pH = 8.5	8.4 ± 0.47	24 ± 4.5	350	1.5 ± 0.18	42 ± 14.4	36
Kidney, pH = 7.4						
HK-J	1.2 ± 0.05	12 ± 2.3	100	0.7 ± 0.05	19 ± 2.9	37
HK-H	1.0 ± 0.07	15 ± 3.2	67	0.5 ± 0.09	23 ± 6.1	22
HK-D	0.5 ± 0.08	19 ± 4.5	26	0.2 ± 0.05	23 ± 2.2	9
Mean	0.9	15	64	0.5	22	23
SD	0.29	2.9	30.3	0.21	1.9	11.4
Kidney heat deactivation, 55° 90 sec						
HK-J	0.7 ± 0.03	12 ± 2.1	58	0.7 ± 0.03	23 ± 4.2	30

Parameter estimates were obtained from the single enzyme Michaelis—Menten equation. Cl_{int} = intrinsic clearance.

formation from SID (Fig. 3B). Kidney microsomes showed the same inhibition pattern as liver microsomes when incubated with *n*-octylamine (data not shown) or with lubrol and methimazole (Fig. 4). Bubbling carbon monoxide through the incubation mixture prior to initiating a reaction with SID failed to elicit significant inhibition (Fig. 4).

Microsomes from B-lymphoblastoid cells expressing CYP1A2, CYP2A6, CYP2C8, CYP2C9-Arg 144, CYP2C19, CYP2D6, CYP2E1, CYP3A4, and CYP4A11 were employed to assess the potential for these enzymes to sulfoxidate SID (0.5 mg protein; 100 μM SID; 30 min). CYP2D6, CYP3A4, and CYP4A11 supported a measurable amount of SOX formation relative to control microsomes. However, these enzymes were relatively inefficient, and did not result in enantiomeric enrichment of SOX.

Correlations between the rates of *R*- and *S*-SOX formation (0.2 mg protein, 100 μM, 20 min) and prototypical catalytic activities of CYPs and FMO or their immunoquantified concentrations in a bank of fourteen human liver microsomal samples are shown in Table 2. For *R*-SOX formation, the only significant correlations were achieved with nicotine *N*-oxide formation, olanzepine *N*-oxide formation, and immunoquantified FMO levels ($r = 0.83$, 0.81, and 0.88; $P < 0.01$), respectively (Fig. 5). *S*-SOX formation rates correlated with taxol 6α-hydroxylation (CYP2C8; $r = 0.70$, $P < 0.01$), dextromethorphan *O*-demethylation (CYP2D6; $r = 0.58$, $P < 0.05$), midazolam 1′-hydroxylation (CYP3A4; $r = 0.87$, $P < 0.01$), and immunoquantified CYP3A4 enzyme levels ($r = 0.62$; $P < 0.05$).

A single protein with an apparent molecular mass of approximately 60 kDa was detected in all human kidney samples examined using an antibody raised against FMO1 (Fig. 6). In our bank of thirteen human kidney microsomal samples, there were highly significant correlations between the rate of formation of total SOX, *R*-SOX, and *S*-SOX and the immunoquantified concentrations of FMO ($r = 0.85$, 0.85, and 0.75; $P < 0.01$), respectively (Fig. 7). The formation rates of *R*-SOX and *S*-SOX also correlated significantly ($r = 0.80$, $P < 0.01$) in human kidney microsomes.

Purified animal FMO1 and FMO2 and human expressed FMO3 Supersomes efficiently catalyzed the oxidation of SID to SOX with an enantioselectivity favoring the *R*-

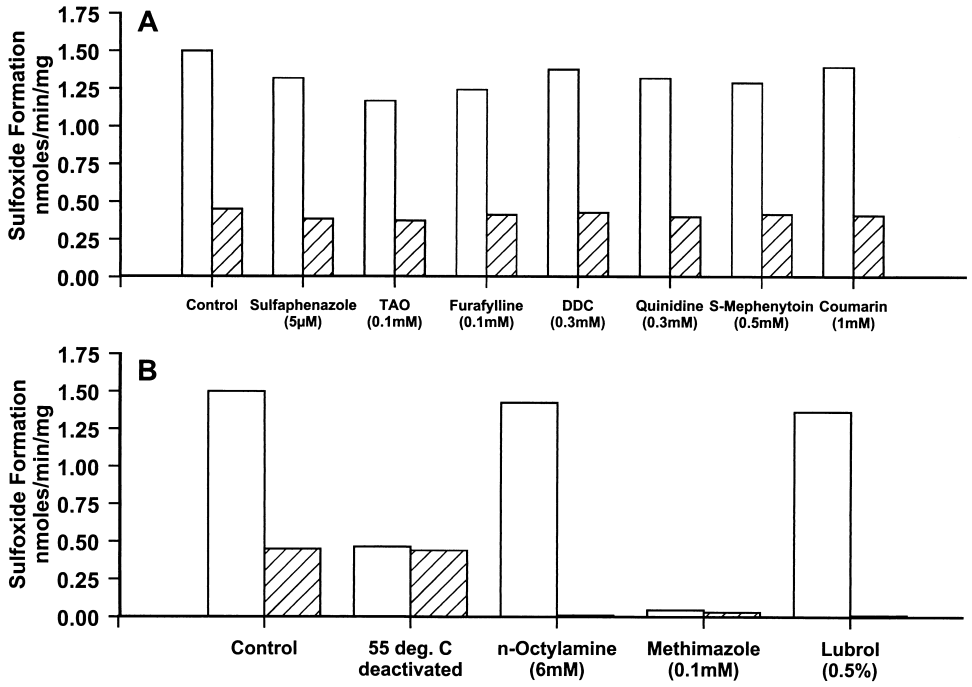

FIG. 3. Effects of selective cytochrome P450 inhibitors (A) and nonselective inhibitors of cytochrome P450 and FMO (B) on *R*-SOX formation (open bars) and *S*-SOX formation (hatched bars) at 30 μM SID with human liver microsomal sample HL-E.

enantiomer at pH 8.5 (Fig. 8). In contrast, FMO5 did not exhibit any appreciable catalytic activity (data not shown). For FMO1 and FMO3 but not FMO2, SOX formation rates reached a maximum at a SID concentration of 50 μM and displayed substrate inhibition at higher substrate concentrations. FMO1 and FMO2 were remarkably stereoselective in the rate of SOX formation with an enantiomeric excess (e.e.) of 98 and 99%, respectively, in favor of the *R*-enantiomer. FMO3 was selective for *R*-SOX production (e.e. = 87%) at 30 μM SID, but was halved at 300 μM (e.e. = 42%) along with a simultaneous reduction in catalytic activity.

DISCUSSION

Sulindac is a NSAID that is employed therapeutically as a racemic mixture of *R*- and *S*-sulfoxides. The sulfoxides are weak inhibitors of cyclooxygenase 1 and 2, but a clinical antiinflammatory response is obtained following *in vivo* reduction to the achiral SID, which is a potent inhibitor of

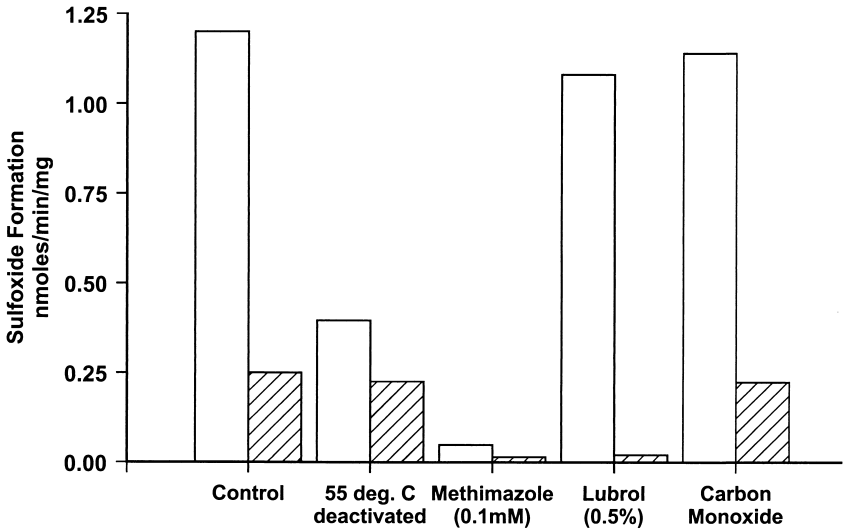

FIG. 4. Effect of nonselective inhibitors of cytochrome P450 and FMO on rates of *R*-SOX (open bars) and *S*-SOX (hatched bars) at 30 μM SID with human kidney microsomal sample HK-J.

TABLE 2. Correlations between total, *R*- and *S*-SOX formation rate (100 μM SID; pH = 7.4) and the immunoquantified protein concentration or selective activities of human cytochrome P450s and FMO in a bank of fourteen (HL-A through HL-N) liver microsomal samples

		Total SOX formation	*R*-SOX formation	*S*-SOX formation
	Total SOX	1.00	0.94*	0.44
	R-SOX		1.00	0.13
	S-SOX			1.00
FMO				
	Immunoquantitation	0.77*	0.88*	−0.08
	Nicotine *N*-oxygenation	0.77*	0.83*	0.05
	Olanzapine *N*-oxygenation	0.76*	0.81*	0.12
CYP1A2				
	Immunoquantitation	0.02	0.16	−0.37
	Caffeine 3-demethylation	−0.02	−0.07	0.13
CYP2A6				
	Immunoquantitation	0.07	−0.10	0.49
	Coumarin 7-hydroxylation	0.05	−0.12	0.50
CYP2C8				
	Immunoquantitation	0.08	−0.02	0.29
	Taxol 6α-hydroxylation	0.07	−0.18	0.70*
CYP2C9				
	Immunoquantitation	−0.02	−0.02	0.01
	Tolbutamide methylhydroxylation	0.34	0.17	0.58†
CYP2C19				
	Immunoquantitation	0.35	0.23	0.43
	S-Mephenytoin 4′-hydroxylation	0.38	0.27	0.41
CYP2D6				
	Immunoquantitation	0.19	0.09	0.34
	Dextromethorphan *O*-demethylation	0.30	0.12	0.58†
CYP2E1				
	Immunoquantitation	−0.35	−0.45	0.18
	Chlorzoxazone 6-hydroxylation	−0.33	−0.42	0.14
CYP3A4				
	Immunoquantitation	0.25	0.05	0.62†
	Midazolam 1′-hydroxylation	0.47	0.21	0.87*
CYP4A				
	Immunoquantitation	−0.35	−0.19	−0.02
	Lauric acid ω-hydroxylation	−0.23	−0.22	−0.11

* $P \leq 0.01$.
† $P \leq 0.05$.

cyclooxygenase 1 and 2 (Fig. 1; [25]). The clearance of SID and SOX *in vivo* is predominately oxidative, with approximately 70% of the dose eliminated in the urine as SOX, sulindac sulfone (SO2), and their conjugates, and the remainder through biliary excretion [1, 4]. The renal clearance of SID is negligible, while that of SOX and SO2 (approx. 7%) is a small percentage of the overall drug clearance, yet renal insufficiency results in an elevated serum SID and SOX concentration [4, 5]. We also observed a distinct enrichment of *R*-SOX in serum and in conjugates of SOX in urine following oral dosing of sulindac. This enrichment is unlikely to reflect enantioselectivity in reduction of SOX to SID because this reaction is effected in the gut by anaerobic microbes or thioredoxin in tissues [26, 27]. Enantioselectivity in the oxidation of SID to SOX and the elimination of SOX via oxidation or conjugation may all contribute to the enantiomeric enrichment noted *in vivo*.

Although SID was shown previously to be a substrate for FMO in both human and animal tissues, the human microsomal enzymes that convert SID to SOX enantioselectively have not been characterized thoroughly, and in particular the relative contribution of CYP and FMO has not been addressed [12, 13]. The FMO family of enzymes consists of five members with distinct tissue selectivity in their expression and activity. FMO1 is the predominate form that is expressed in the kidneys of humans, displays a high enantioselectivity towards *p*-tolyl methyl sulfide, and could be responsible for the renal sparing properties of sulindac [9, 12, 16]. FMO2 is found in lung tissue of humans and is reported to be expressed as a truncated inactive protein in all but a small group of people of African descent [28]. Therefore, FMO2 would not contribute to the overall disposition of sulindac in humans. FMO3, FMO4, and FMO5 have been identified in the liver, with FMO3 the predominate protein expressed [29, 30]. The oxidation of

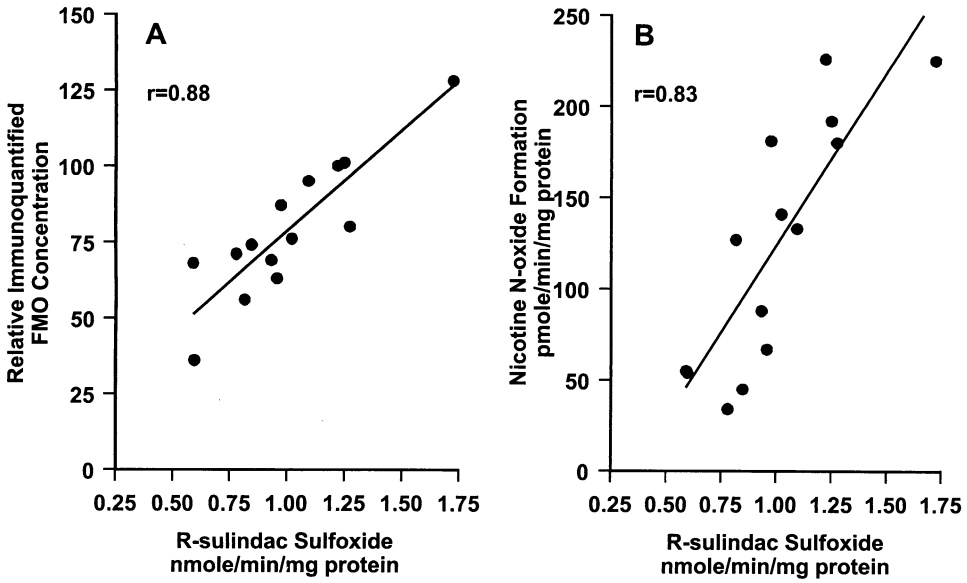

FIG. 5. Correlations between the rates of formation of *R*-SOX and (A) immunoquantified FMO or (B) nicotine *N*-oxide formation rates in fourteen human liver microsomal samples.

alkyl–aryl sulfides by CYP also has been noted. For example, SID was a poor substrate for purified rat liver CYPs, but after treatment with phenobarbital the microsomal oxidation by CYPs increased [13]. Therefore, we have examined the relative contribution of FMO and CYP enzymes to this chiral oxidative pathway in the human liver and kidney, and with individual proteins.

Human liver and kidney microsomes readily oxidized SID with a high level of stereoselectivity (Table 1 and Fig. 2) in favor of *R*-enantiomer production, which is similar to the observed pattern in human serum. Established inhibitors of human CYPs were incapable of inhibiting the rate of sulfoxidation of SID, with the exception of furafylline (CYP1A2) and troleandomycin (CYP3A4), which slightly reduced catalytic activity. This modest inhibition may be due to the preincubation conditions producing thermal strain on the microsomal FMO system prior to reaction initiation. cDNA-expressed CYP2D6, CYP3A4, and CYP4A11 exhibited a measurable rate of SID sulfoxidation, but the turnover was relatively low. Correlations between *S*-SOX formation rate and taxol 6α-hydroxylation (CYP2C8) or dextromethorphan *O*-demethylation (CYP2D6) in a panel of human liver microsomes did reach significance (Table 2), but the corresponding selective inhibitors sulfaphenazole and quinidine did not reduce catalytic activity effectively. The correlations between *S*-SOX and midazolam 1′-hydroxylation and immunoquantified CYP3A4 levels (r = 0.87 and 0.62) were not high enough to be predictive, and the relationships did not pass through the origin. The *S*-SOX formation rates also correlated with total CYP450 content (r = 0.80), which may reflect the high relative abundance of CYP3A4. However, CYPs are known to generate reactive oxygen species in microsomal preparations containing NADPH, which may result in nonenzymatic sulfoxidation of SID and, in turn, result in the observed correlation with total CYP. Nevertheless, including catalase or superoxide dismutase, to curtail reactive oxygen production, in NADPH-supplemented liver microsomes had little effect on SOX formation (data not shown). Lipid peroxidase activity generating active oxygen species appears to be minimal, due to the lack of effect of oxygen scavengers and the loss of *S*-SOX formation with the inhibitor *n*-octylamine and membrane solubilization with lubrol. Another possible influence on the overall stereoselectivity is reduction of SOX to the sulfide by the microsomal fraction. Human liver microsomal preparations HL-A, HL-D, and HL-E (0.2 mg) were incubated with 30 μM SOX and 1 mM NADPH for 30 min. The microsomes exhibited no detectable formation of SID, but produced a small amount of the sulfone metabolite (data not shown). Thus, there appears to be some evidence for a minor contribution of CYP, and CYP3A4 in particular, to the sulfoxidation of SID to *S*-SOX. In general, CYPs do not appear to make a major contribution to the oxidation of SID, although it remains possible that CYPs may become significant in individuals exposed to potent inducers.

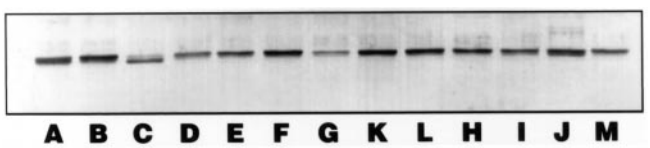

FIG. 6. Western blot (9% SDS–PAGE) of human kidney microsomes probed with an antibody raised against rabbit liver FMO1. See text for details.

Purified animal forms FMO1 and FMO2 and human expressed FMO3 readily oxidized SID with a preference for

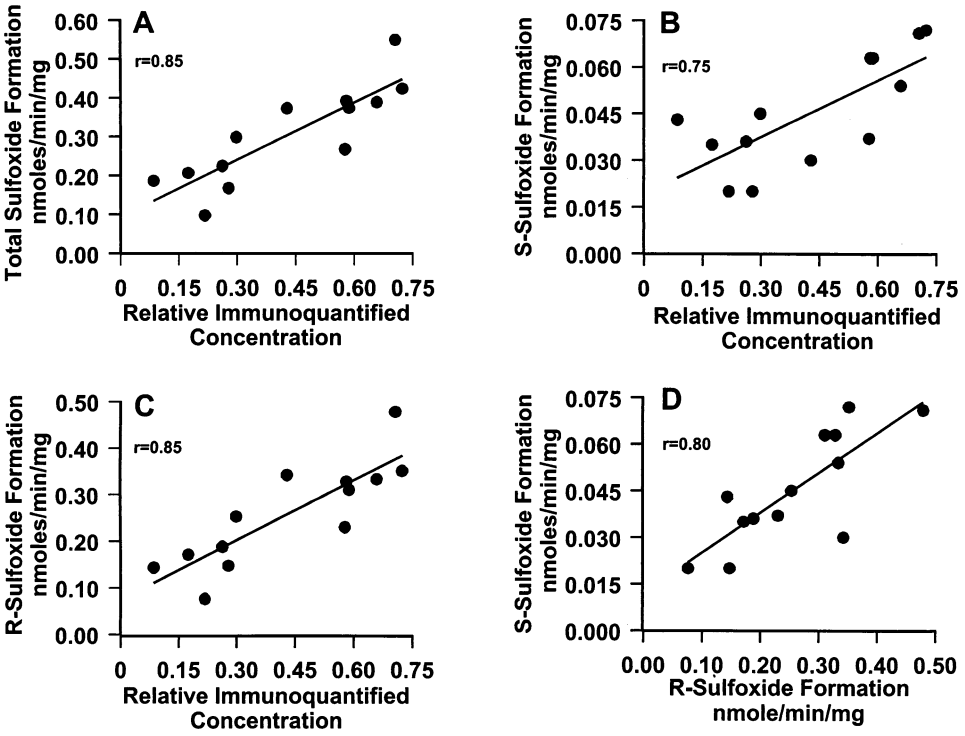

FIG. 7. Correlations between the rates of formation of total SOX, *S*-SOX, *R*-SOX, and immunoquantified FMO levels in thirteen human kidney microsomal samples.

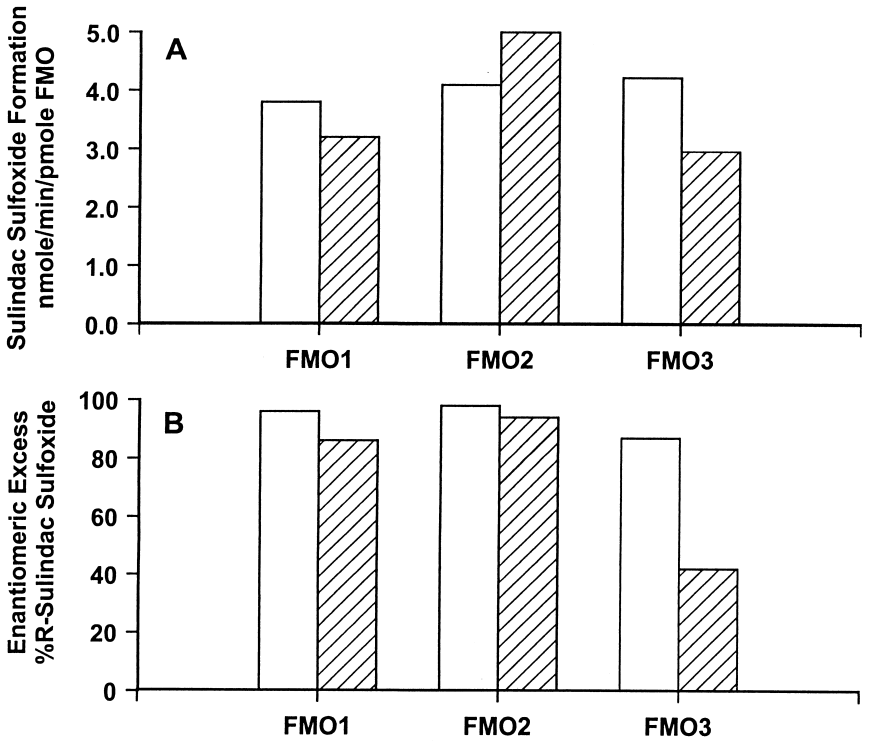

FIG. 8. (A) Rate of formation of total SOX by purified mini-pig FMO1 and rabbit lung FMO2 and cDNA-expressed human liver FMO3, pH = 8.5, at 30 μM (open bars) and 300 μM (hatched bars) SID. (B) Corresponding percent of *R*-SOX enantiomeric excess.

R-SOX formation, as did the microsomes prepared from human liver and kidney tissue. In particular, hepatic microsomes and FMO3, the major hepatic FMO, formed SOX with similar enantiomeric excesses of 85%. Similarly, renal microsomes and the principal renal isoform, FMO1, formed SOX with comparable enantiomeric excesses of 97%. Incubations performed at pH 8.5 displayed a substantial increase in the V_{max} of *R*-SOX formation, which is characteristic of FMO-mediated reactions [31]. This pH dependence presumably reflects amplification of the base-catalyzed decomposition of the C-4α hydroxyperoxide flavin, which subsequently increases the maximal reaction rate [32]. The substrate concentration dependence of SID in microsomal preparations exhibited a pattern consistent with substrate inhibition, particularly for *R*-SOX, at concentrations greater than 100 μM (Fig. 2). Therefore, kinetic parameters were determined with substrate concentrations from 1 to 200 μM SID. Importantly, this pattern was also exhibited by expressed FMO3. A possible explanation for this phenomenon is substrate insolubility; however, after mild heat deactivation of tissue microsomes or cDNA-expressed FMO3, the effect was less pronounced (Fig. 3B) and was completely absent with renal microsomes. Thus, substrate inhibition may be a property of FMO3, but this has not been noted previously.

The good correlation between the rate of *R*-SOX formation and the prototypical FMO-mediated reactions of nicotine and olanzepine *N*-oxidation [18, 21] and immunoquantified FMO3 (Fig. 5 and Table 2) reinforces the conclusion that this reaction is mediated principally by this enzyme. *S*-SOX activity did not correlate with *R*-SOX, nicotine *N*-oxide formations, or FMO levels (Table 2). Perhaps this reflects the presence of other liver FMOs (FMO4) that have different substrate selectivities and/or different interactions with the antibody used in quantitation. In contrast, the human kidney bank produced highly significant correlations between *R*-SOX, *S*-SOX activities, and FMO immunoquantified levels (Fig. 7). The human kidney is known to express mostly FMO1, and, therefore, these good correlations were expected.

The FMO substrates methimazole and *n*-octylamine [32, 33] displayed differing inhibitory effects on SID oxidation rates with microsomal preparations. Whereas methimazole was a powerful nonstereoselective inhibitor of sulfoxidation, *n*-octylamine was completely and selectively inhibitory to *S*-SOX formation. The complete inhibition observed with methimazole lends support to the conclusion that *R*- and *S*-sulfoxidation of SID are exclusively FMO-mediated reactions. *n*-Octylamine is also known to be a potent nonselective CYP inhibitor, but its lack of inhibition by other CYP inhibitors suggests that it is not acting in this capacity. Detergent solubilization with lubrol resulted in the same inhibition pattern as *n*-octylamine, but mild heat inactivation of hepatic and renal microsomes selectively impaired *R*-SOX activity. Solubilization of enzyme from the microsomal membrane generally does not impede the rates for FMO-catalyzed reactions [17]; however, for SID it appears to do so. The weight of evidence obtained with human renal microsomes suggests that these inhibitors and partial heat inactivation may be modulating different conformations of human FMO1 and/or its microsomal environment and may modify prochiral recognition by FMO1.

In the human liver multiple isoforms of FMO are present, with the potential for differences in catalytic activities and substrate specificity [30], and thus the mechanism underlying the effects of inhibitors and heat deactivation may be more complex. Despite the presence of multiple active enzymes, concentration dependence with a substrate such as SID may not necessarily display a multiple enzyme pattern unless a K_m difference of 10-fold or more exists between the isozymes. A single enzyme model best described *R*-SOX and *S*-SOX formation rates, but their activities correlated poorly with each other, suggesting that different enzymes do indeed contribute to these reactions. The principal FMO in the human liver is FMO3, but there was a higher enantiomeric excess of *R*-SOX with cDNA-expressed FMO3 incubations than with liver microsomes. The use of pH, heat deactivation, detergent membrane solubilization, and *n*-octylamine with SID may assist in characterizing the relative contributions of other human isozymes, such as FMO4, once this enzyme is characterized more completely [30].

A prototypic probe for FMO is *p*-tolyl methyl sulfide, which has been instrumental in revealing differences in catalytic activities among various human tissues and animal FMO homologues [13, 14, 16, 17, 20]. A disadvantage to using *p*-tolyl methyl sulfide as an FMO probe is that it is also a substrate for CYPs, and therefore microsomal membranes must be solubilized to focus on FMO oxidation [13, 14]. Using this approach, it was shown that cDNA-expressed FMO2 and detergent-solubilized rabbit lung microsomes achieved a high degree of agreement in stereoselective production of *R*-*p*-tolyl methyl sulfoxide [16]. However, our data indicate that cDNA-expressed FMO3 microsomes did not compare favorably with detergent-solubilized human liver microsomes in stereochemical sulfoxide production from SID (Fig. 4). As a specific FMO substrate, SID can be employed to quantify catalytic activity in human kidney, liver, and lung, and therefore may be superior to *p*-tolyl methyl sulfide because solubilization is unnecessary.

In summary, human tissues and individual FMOs oxidized SID stereoselectively and the major product formed was *R*-SOX, which is consistent with the observation of enrichment of this enantiomer in human serum and urine. The oxidation of SID was entirely FMO dependent, with little if any CYP involvement. The pro-*R* and pro-*S* SID interactions with FMOs are distinguishable by raising pH, by heat inactivation, and by detergent membrane solubilization.

This work was supported by NIH Grants AG07631 (S. D. H.) and GM43511 (A. E. R.)

References

1. Hucker HB, Stauffer SC, White SD, Rhodes RE, Arison BH, Umbenhauer ER, Bower RJ and McMahon FG, Physiologic disposition and metabolic fate of a new anti-inflammatory agent, *cis*-5-fluoro-2-methyl-1-[*p*-(methylsulfinyl)-benzylidenyl]-indene-3-acetic acid in the rat, dog, rhesus monkey, and man. *Drug Metab Dispos* **1:** 721–736, 1973.
2. Duggan DE, Hooke KF, Risley EA, Shen TY and Van Arman CG, Identification of the biologically active form of sulindac. *J Pharmacol Exp Ther* **201:** 8–13, 1977.
3. Swanson BM, Boppana VK, Rickards NJ, Holms GI, Davies RO and Huber PB, Initial clinical studies of the bioactive sulfide metabolite of sulindac. *Clin Res* **30:** 477–487, 1982.
4. Sitar DS, Owen JA, MacDougall B, Hunter T and Mitenko PA, Effects of age and disease on the pharmacokinetics and pharmacodynamics of sulindac. *Clin Pharmacol Ther* **38:** 228–234, 1985.
5. Hall SD, Hamman MA, Murray MD and Brater DC, Effects of age and renal function on sulindac disposition in humans. *FASEB J* **7:** A482, 1993.
6. Gibson TP, Dobrinska MR, Lin JH, Entwistle LA and Davies RO, Biotransformation of sulindac in end-stage renal disease. *Clin Pharmacol Ther* **42:** 82–88, 1987.
7. Hamman MA and Hall SD, Sulindac sulfoxide (SOX) enantiomer disposition. *FASEB J* **7:** A482, 1993.
8. Whelton A, Stout RL, Spilman PS and Klassen DK, Renal effects of ibuprofen, piroxicam and sulindac in patients with asymptomatic renal failure: A prospective randomized, crossover comparison. *Ann Intern Med* **112:** 568–576, 1990.
9. Bunning RD and Barth WF, Sulindac: A potentially renal-sparing nonsteroidal anti-inflammatory drug. *JAMA* **248:** 2864–2867, 1982.
10. Murray MD and Brater DC, Renal toxicity of the nonsteroidal anti-inflammatory drugs. *N Engl J Med* **310:** 563–572, 1984.
11. Abraham PA and Keane WF, Glomerular and interstitial disease induced by nonsteroidal anti-inflammatory drugs. *Am J Nephrol* **4:** 1–6, 1984.
12. Eriksson LO and Boström H, Deactivation of sulindac sulfide by human renal microsomes. *Pharmacol Toxicol* **62:** 177–183, 1988.
13. Waxman DJ, Light DR and Walsh C, Chiral sulfoxidations catalyzed by rat liver cytochromes P-450. *Biochemistry* **21:** 2499–2507, 1982.
14. Light DR, Waxman DJ and Walsh C, Studies on the chirality of sulfoxidation catalyzed by bacterial flavoenzyme cyclohexanone monooxygenase and hog liver flavin adenine dinucleotide containing monooxygenase. *Biochemistry* **21:** 2490–2498, 1982.
15. Hines RN, Cashman JR, Philpot RM, Williams DE and Zeigler DM, The mammalian flavin-containing monooxygenases: Molecular characterization and regulation of expression. *Toxicol Appl Pharmacol* **125:** 1–6, 1994.
16. Rettie AE, Lawton MP, Sadeque AJM, Meier GP and Philpot RM, Prochiral sulfoxidation as a probe for multiple forms of the microsomal flavin-containing monooxygenase: Studies with rabbit FMO1, FMO2, FMO3 and FMO5 expressed in *Escherichia coli*. *Arch Biochem Biophys* **311:** 369–377, 1994.
17. Sadeque AJM, Eddy AC, Meier GP and Rettie AE, Stereoselective sulfoxidation by human flavin-containing monooxygenase. Evidence for catalytic diversity between hepatic, renal, and fetal forms. *Drug Metab Dispos* **20:** 832–839, 1992.
18. Ring BJ, Catlow J, Lindsay TJ, Gillespie T, Roskos LK, Cerimele BJ, Swanson SP, Hamman MA and Wrighton SA, Identification of the human cytochromes P450 responsible for the *in vitro* formation of the major oxidative metabolites of the antipsychotic agent olanzapine. *J Pharmacol Exp Ther* **276:** 658–666, 1996.
19. Lowry OH, Rosebrough NJ, Farr AL and Randall RJ, Protein measurement with the Folin phenol reagent. *J Biol Chem* **193:** 265–275, 1951.
20. Sadeque AJM, Thummel KE and Rettie AE, Purification of macaque liver flavin-containing monooxygenase: A form of the enzyme related immunochemically to an isozyme expressed selectively in adult human liver. *Biochim Biophys Acta* **1162:** 127–134, 1993.
21. Cashman JR, Park SB, Yang ZC, Wrighton SA, Jacob P III and Benowitz NL, Metabolism of nicotine by human liver microsomes: Stereoselective formation of *trans*-nicotine *N′*-oxide. *Chem Res Toxicol* **5:** 639–646, 1992.
22. Wrighton SA, VandenBranden M, Stevens JC, Shipley LA, Ring BJ, Rettie AE and Cashman JR, *In vitro* methods for assessing human hepatic drug metabolism: Their use in drug development. *Drug Metab Rev* **25:** 453–484, 1993.
23. McManus ME, Stupans I, Burgess W, Koenig JA, Hall PM and Birkett DJ, Flavin-containing monooxygenase activity in human liver microsomes. *Drug Metab Dispos* **15:** 256–261, 1987.
24. Segal IH, *Enzyme Kinetics*. John Wiley, New York, 1975.
25. Rider NL, Pinto D, Covington M, Orwat MJ, Giannors J, Nurnberg S, Dowling R, Davis JP, Williams JM, Trzaskos JM and Copeland RA, Comparative effects of selective cyclooxygenase 1 and cyclooxygenase 2 inhibitors on myeloperoxidase and 3 α-hydroxysteroid dehydrogenase. *J Enzyme Inhib* **10:** 73–79, 1996.
26. McLane KE, Fisher J and Ramakrishnan K, Reductive drug metabolism. *Drug Metab Rev* **14:** 741–799, 1983.
27. Anders MW, Ratnayake JH, Hanna PE and Fuchs JA, Involvement of thioredoxin in sulfoxide reduction by mammalian tissues. *Biochem Biophys Res Commun* **97:** 846–851, 1980.
28. Dolphin CT, Beckett DJ, Janmohamed A, Cullingford TE, Smith RL, Shephard EA and Phillips IR, The flavin-containing monooxygenase 2 gene (*FMO2*) of humans, but not of other primates, encodes a truncated, nonfunctional protein. *J Biol Chem* **273:** 30599–30607, 1998.
29. Overby LH, Carver GC and Philpot RM, Quantitation and kinetic properties of hepatic microsomal and recombinant flavin-containing monooxygenases 3 and 5 from humans. *Chem Biol Interact* **106:** 29–45, 1997.
30. Phillips IR, Dolphin CT, Clair P, Hadley MR, Hutt AJ, McCombie RR, Smith RL and Shepard EA, The molecular biology of the flavin-containing monooxygenases of man. *Chem Biol Interact* **96:** 17–32, 1995.
31. Gold MS and Zeigler DM, Dimethylaniline *N*-oxidase and aminopyrine *N*-demethylase activities of human liver tissue. *Xenobiotica* **3:** 179–189, 1973.
32. Ziegler DM, Flavin-containing monooxygenases: Catalytic mechanism and substrate specificities. *Drug Metab Rev* **19:** 1–32, 1988.
33. Ziegler DM, Recent studies on the structure and function of multisubstrate flavin-containing monooxygenases. *Annu Rev Pharmacol Toxicol* **33:** 179–199, 1993.